

Direct observation of charge inversion by multivalent ions as a universal electrostatic phenomenon

K. Bester, M. A. G. Zevenbergen, H. A. Heering, and S. G. Lemay
 Kavli Institute of Nanoscience, Delft University of Technology, 2628 CJ Delft, The Netherlands
 (Dated: January 27, 2020)

We have directly observed reversal of the polarity of charged surfaces in water upon the addition of tri- and quadrivalent ions using atomic force microscopy. The bulk concentration at which charge inversion reversibly occurs depends only very weakly on the chemical composition, surface structure, size and lipophilicity of the ions, but is dominated by their valence. These results support the theoretical proposal that spatial correlations between ions are the driving mechanism behind charge inversion.

Understanding screening due to mobile ions in liquid is a key theme of such diverse fields as polymer physics, nanodynamics, colloid science and molecular biophysics. Screening by multivalent ions in particular results in several counter-intuitive phenomena, for example attraction between like-charged macromolecules such as DNA [1] and actin filaments [2]. Similarly, the electrophoretic mobility of charged colloids reverses sign upon introducing a sufficient concentration of multivalent ions in solution [3, 4], a phenomenon known as charge inversion.

The conventional paradigm for describing screening in liquid divides the screening ions into two components: (1) the so-called Stern layer, consisting of ions bound to the surface, and (2) a diffuse component described by the Poisson-Boltzmann (PB) equation that decays exponentially with distance far from the charged object. Charge inversion can be accounted for by introducing a "chemical" binding constant that reduces the free energy of multivalent ions situated in the Stern layer, reflecting an assumed specific interaction between these ions and the surface being screened. This chemical binding constant is expected to depend on properties of the ions such as their size, chemical composition, surface structure, lipophilicity and valence. While this approach has been successful in describing experimental data [3, 5, 6, 7], it usually provides little insight into the underlying binding mechanism and lacks significant predictive power.

A universal mechanism for charge inversion based predominantly on electrostatic interactions has been proposed [8]. It was noted that the predicted chemical potential of the Stern layer can be significantly lowered if spatial correlations between discrete ions are accounted for. At room temperature, the loss of entropy entailed by the formation of a highly correlated ionic system is substantial. For multivalent counterions and sufficiently high surface charge densities, however, this is more than compensated by the corresponding gain in electrostatic energy, leading to charge inversion [9]. To date, these theories have remained untested by experiments.

Here we present direct measurements of charge inversion and its dependence on the properties of the screening ions. Using an atomic force microscope (AFM), we

measured the force between two oppositely charged surfaces. This approach circumvents the main limitations of previous measurements, namely, reliance on modelling of hydrodynamic effects [3, 4] and the need to disentangle phenomena at two similarly-charged surfaces [5, 7]. We observe that in the presence of a sufficiently high concentration of tri- and quadrivalent ions, the force reversibly changes sign. The bulk concentration at which charge inversion occurs, the so-called charge-inversion concentration c_0 , depends almost exclusively on the valence of the ions, consistent with the universal predictions of the ion-correlation theories.

Positively chargedamine-terminated surfaces were prepared under argon atmosphere by immersing silicon wafers with 200–500 nm thermally-grown oxide in a 0.1% solution of 1-trichlorosilyl-11-cyanoundecane (Gleat) in toluene for 30 minutes, then in a 20% solution of Red Al (Sigma-Aldrich) in toluene for 5 hours. Negatively charged surfaces were prepared by gluing 10 nm diameter silica spheres (G. Kisker Gehr) with epoxy resin to AFM cantilevers (Thermofischer Microscope Microlevers) using a method similar to that of Ducker et al [10], as illustrated in Fig. 1(a).

Using a Digital Instrument NanoScope IV AFM, force spectroscopy measurements were performed yielding the force F on the silica bead versus the bead-surface separation d [10]. The spring constant of the cantilevers was 0.03 N/m, as given by the manufacturer. Care was taken to minimize the scattering of light from the surface so as to eliminate interference effects.

At separations d greater than the Debye length of the solution, the force decays exponentially with d :

$$F = F_0 \exp(-d/d_0); \quad d > d_0 \quad (1)$$

The parameter F_0 is proportional to the so-called renormalized surface charge densities of both the silica bead and the amine-terminated surface, σ_b and σ_s respectively. The values of $\sigma_{b,s}$ are related by the PB equation to the net surface charge densities σ_b and σ_s (including both the bare surface charge and the charge in the Stern layer). At low net surface charge densities $|\sigma_{b,s}| < \sigma_{max}$, the renormalized charge densities are simply equal to the

net charge densities: $\gamma_{bs} = \gamma_{bs}^0$. Here $\gamma_{max} = 4 kT/e$, where k is the Boltzmann constant, T is the temperature, ϵ is the dielectric constant of water and e is the electron charge. At higher net charge densities, γ_{bs} saturates at γ_{max} . Because we use oppositely charged surfaces and $Z \geq 1$ electrolytes, where Z is the valence of the multivalent ions, only one of the surfaces is affected by the introduction of multivalent ions. The other surface thus plays the role of a constant probe. Near charge inversion, F_0 is thus proportional to the net surface charge density of the surface being screened by multivalent ions, γ_b or γ_s , and the sign of the force yields unambiguously the polarity of this net surface charge.

For $d < \lambda_D$, the PB equation predicts a more complicated form than Eq. (1). In addition, van der Waals forces, regulation of the surface charge and depletion forces can become important. We therefore concentrate our analysis on the regime $d > \lambda_D$.

Three positive trivalent ions, Lanthanum La^{3+} , ruthenium (III) hexammine $[\text{Ru}(\text{NH}_3)_6]^{3+}$ and cobalt (III) sepulchrate $[\text{CoC}_{12}\text{H}_{30}\text{N}_8]^{3+}$ were investigated. La^{3+} is an elemental metal ion with a first hydration shell consisting of 8–9 water molecules (radius of the complex 398 pm [11, 12, 13, 14]). $[\text{Ru}(\text{NH}_3)_6]^{3+}$ contains a Ru (III) core with six NH_3 groups around it (radius 364 pm [11, 12, 13]). $[\text{CoC}_{12}\text{H}_{30}\text{N}_8]^{3+}$ is a caged cobalt complex with CH_2 groups exposed to the water environment (radius 445 pm [15]), making it less hydrophilic than the other two.

Figure 1 shows the measured force-distance relation $F(d)$ as a function of multivalent ion concentration c for the multivalent salts LaCl_3 (b), $[\text{CoC}_{12}\text{H}_{30}\text{N}_8]^{3+}$ (c) and $[\text{Ru}(\text{NH}_3)_6]^{3+}$ (d). A force measurement with only supporting electrolyte (LaCl_3 : [16], $[\text{CoC}_{12}\text{H}_{30}\text{N}_8]^{3+}$ and $[\text{Ru}(\text{NH}_3)_6]^{3+}$: [17]) was first performed (black squares), showing an attractive interaction between the surfaces. Solutions with increasing concentrations of multivalent ions in the monovalent supporting electrolyte were then pumped through the AFM fluid cell of 50 μl volume at a rate 0.15–0.2 ml/min for at least 5 minutes per solution. This allowed the surface to equilibrate with the electrolyte and insured that c was not influenced when large numbers of ions screened the surface. Consecutive measurements of $F(d)$ at multivalent ion concentrations $c = 10 \text{ M}, 100 \text{ M}$ and 1 mM are shown in Fig. 1. At the end of the experiment, the measurement with $c = 10 \text{ M}$ was repeated (red open circles). The $[\text{CoC}_{12}\text{H}_{30}\text{N}_8]^{3+}$ and $[\text{Ru}(\text{NH}_3)_6]^{3+}$ measurements were carried out consecutively using the same silica bead.

We interpret these observations as follows. The positive multivalent ions adsorb on the negative silica bead, reducing γ_b and thus the magnitude of the force. Near 1 mM, the screening charge in the Stern layer overcompensates for the bare surface charge; γ_b becomes positive and the force becomes repulsive. The last measurement with $c = 10 \text{ M}$, which shows a recovery to the force measured at $c = 0$, indicates that the multivalent ions are desorbed from the surface.

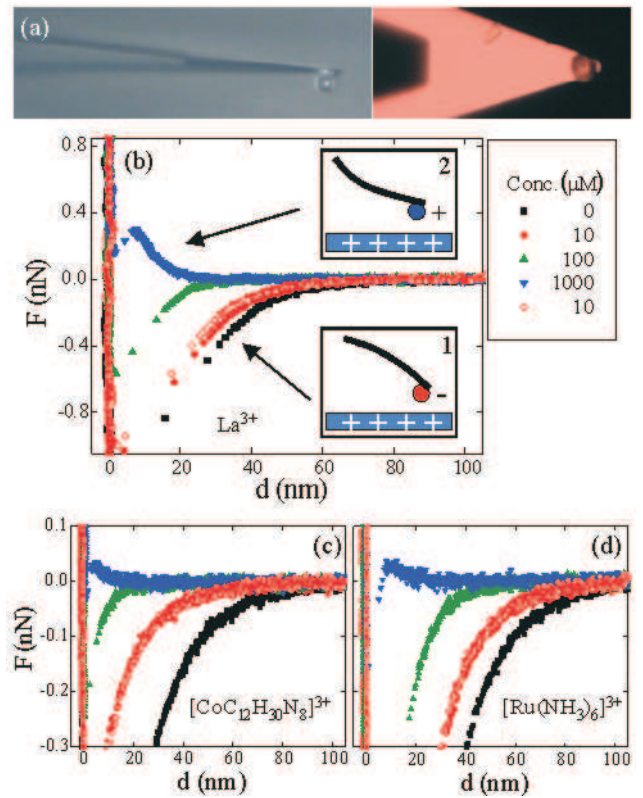


FIG. 1: (color) (a) Optical micrographs of the side (left) and top (right) of a cantilever with a silica sphere. Force versus separation measurements in different concentrations of (b) LaCl_3 , (c) and (d) $[\text{Ru}(\text{NH}_3)_6]^{3+}$. Insets illustrate schematically the attractive (1) and repulsive (2) forces between the silica bead and the amine-terminated surface. The legend applies to all three graphs.

sured at the beginning of the experiment, indicates that charge inversion reflects reversible equilibrium between the surface and the bulk electrolyte.

To further compare the charge-inversion concentration of the same surface with different multivalent ions, the force for $d > \lambda_D$ was fitted to Eq. 1. Because it is difficult to accurately fit the Debye length when the force is very small, its value was fitted for the curve with $c = 0$ and corrected using the standard expression for F_0 for the cases $c > 0$.

Figure 2(a) shows the fitted normalized force extrapolated to zero separation, $F_{N0}(c) = F_0(c)/F_0(0)$, for the $[\text{CoC}_{12}\text{H}_{30}\text{N}_8]^{3+}$ and $[\text{Ru}(\text{NH}_3)_6]^{3+}$ data of Fig. 1(c,d). Similarly, Fig. 2(b) shows $F_{N0}(c)$ for consecutive measurements using the same silica bead on La^{3+} (data from Fig. 1(b)) and $[\text{Ru}(\text{NH}_3)_6]^{3+}$ (Fig. 1(d) curves not shown). We estimate the charge-inversion concentration c_0 by linearly interpolating between the data points immediately above and below $F_N = 0$ on the lin-log scale. In both sets of measurements, the observed values of c_0 differ by a factor 2. More generally, we find that the charge-inversion concentrations of silica for the three chemically different

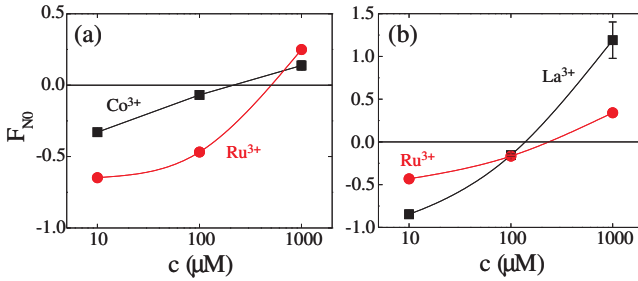


FIG. 2: Normalized force extrapolated to zero separation obtained from fits to Eq. (1), versus multivalent ion concentration c for (a) $\text{CoC}_{12}\text{H}_{30}\text{N}_8\text{C}_{13}$ (squares) and $\text{Ru}(\text{NH}_3)_6\text{C}_{13}$ (circles) and for (b) La^{3+} (squares) and $\text{Ru}(\text{NH}_3)_6\text{C}_{13}$ (circles). In each case the data were obtained consecutively using the same silica bead. Lines are guides to the eye.

trivalent ions La^{3+} , $\text{Ru}(\text{NH}_3)_6^{3+}$ and $[\text{CoC}_{12}\text{H}_{30}\text{N}_8]^{3+}$ differ by at most a factor of 2.1, as summarized in Table I. This is comparable to the variation observed between measurements for the same ion and pH using different, nominally identical beads and surfaces. Although the charge-inversion concentrations of the three positive trivalent ions are similar, there are differences in the observed $F(d)$ curves. In particular, La^{3+} is less effective in reducing the absolute force at low concentrations, but the magnitude of the force for $c = c_0$ is largest for La^{3+} .

Figure 3 shows measurements where the same anion-terminated surface was consecutively charge inverted by a molecule in two different charge states, iron (II) hexacyanide $[\text{Fe}(\text{CN})_6]^{4-}$ (radius 443 pm) and iron (III) hexacyanide $[\text{Fe}(\text{CN})_6]^{3-}$ (radius 437 pm) [11, 12, 13], ensuring that essentially the only difference between the two measurements is the valence of the ions [18]. Figure 3(c) shows the F_{N0} for both ions as a function of the concentration. The charge-inversion concentrations for the two ions differ by a factor ~50.

Measurements using $[\text{Fe}(\text{CN})_6]^{4-}$ and ruthenium (II) hexacyanide $[\text{Ru}(\text{CN})_6]^{4-}$ (radius 456 pm [11, 12, 13, 19]), two ions with nearly identical chemical groups exposed to solution and differing only by their core atom, gave nearly identical $F(d)$ curves at all concentrations.

Two divalent ions, calcium Ca^{2+} and magnesium Mg^{2+} (radii of 388 and 348 pm, respectively [11, 12, 13, 14]) did not show charge inversion at a concentration of 1 mM on a silica bead that showed charge inversion at 1 mM La^{3+} . Thus divalent ions, if they can charge invert a silica bead at all, do so at higher concentrations than trivalent ions. Concentrations higher than 1 mM were not investigated in this study because the Debye length then becomes so short that effects such as van der Waals forces mask the electrostatic interaction between the surfaces.

Additional experiments were performed with positively charged surfaces made by chemically modifying a silicon dioxide surface with 3-aminopropyltriethoxysilane (APTES) and by adsorbing poly-L-lysine on mica. Key

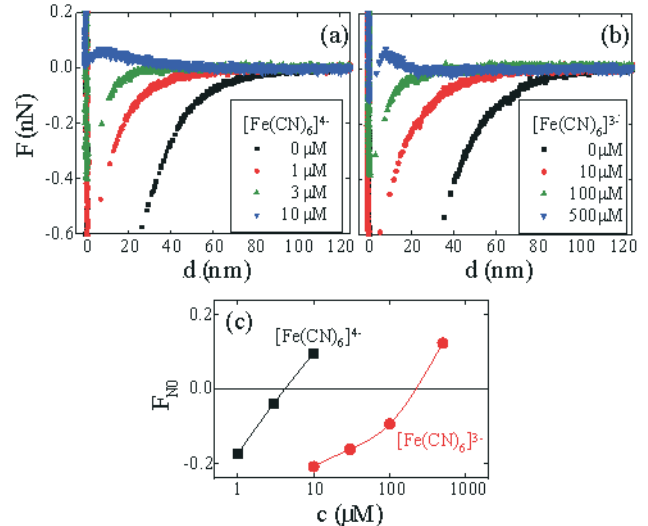


FIG. 3: (color) Force versus separation measurements in different concentrations of (a) $\text{K}_4\text{Fe}(\text{CN})_6$ and (b) $\text{K}_3\text{Fe}(\text{CN})_6$. (c) Normalized force at zero separation versus multivalent ion concentration c for $\text{K}_4\text{Fe}(\text{CN})_6$ (squares) and $\text{K}_3\text{Fe}(\text{CN})_6$ (circles). Lines are guides to the eye.

results are summarized in Table I

In terms of a chemical binding description, our measurements indicate that the binding constants for La^{3+} , $\text{Ru}(\text{NH}_3)_6^{3+}$ and $[\text{CoC}_{12}\text{H}_{30}\text{N}_8]^{3+}$ on silica differ by at most a factor ~2, despite the fact that these ions have significantly different chemical composition, surface structure, size and lipophilicity. The binding constant differs at least 10-fold for the same molecule in two different charge states on anion-terminated surfaces. These observations strongly suggest that specific chemical interactions are not responsible for charge inversion in our measurements and that the mechanism for adsorption is predominantly electrostatic.

For comparing our results with ion-correlation theories we employ the formalism of Shklovskii [9], in which the multivalent counterions in the Stern layer are assumed to form a strongly correlated liquid with short-range correlations resembling those of a Wigner crystal. This theory provides a simple analytical prediction for the charge-inversion concentration:

$$c_0 = (\text{bare}^{-Z} \text{ew}) \exp(-c/kT) \quad (2)$$

Here bare is the bare surface charge density and c is the chemical potential of the ions in the Stern layer. The latter can be approximated by the value for a Wigner crystal: $c / \text{bare}^{1/2} Z^{3/2}$. In the calculations we use the full expression for c [9]. The parameter w has units of length and reflects additional microscopic details not explicitly included in the theory.

Qualitatively this theory is in good agreement with our observations. The predictions that charge inversion is a general equilibrium effect and q depends very sensitively

TABLE I: Summary of measurements in which the same surface was charged inverted by two different ions.

surface	probe	supp. elect.	ion (1)	ion (2)	$c_0^{(1)}$ (M)	$c_0^{(2)}$ (M)	$c_0^{(\text{high})} = c_0^{(\text{low})}$
APTES	silica bead	[20]	$[\text{Fe}(\text{CN})_6]^{4-}$	$[\text{Fe}(\text{CN})_6]^{3-}$	13	170	13
chlorosilane	silica bead	[18]	$[\text{Fe}(\text{CN})_6]^{4-}$	$[\text{Fe}(\text{CN})_6]^{3-}$	4	200	50
APTES	silica bead	[20]	$[\text{Ru}(\text{CN})_6]^{4-}$	$[\text{Fe}(\text{CN})_6]^{4-}$	11	13	1.2
silica bead	APTES	[20]	La^{3+}	$[\text{Ru}(\text{NH}_3)_6]^{3+}$	560	730	1.3
silica bead	poly-L-lysine	[16]	$[\text{CoC}_{12}\text{H}_{30}\text{N}_8]^{3+}$	La^{3+}	190	120	1.6
silica bead	poly-L-lysine	[16]	$[\text{CoC}_{12}\text{H}_{30}\text{N}_8]^{3+}$	La^{3+}	170	180	1.1
silica bead	chlorosilane	[16]	La^{3+}	$[\text{Ru}(\text{NH}_3)_6]^{3+}$	130	210	1.6
silica bead	chlorosilane	[17]	$[\text{CoC}_{12}\text{H}_{30}\text{N}_8]^{3+}$	$[\text{Ru}(\text{NH}_3)_6]^{3+}$	210	450	2.1
poly-L-lysine	silica bead	[20]	$[\text{Ru}(\text{CN})_6]^{4-}$		22		

on Z but lacks dependence on the chemical structure of the ions agree with our measurements.

In order to perform a more quantitative test of Eq. (2), we calculate the bare surface charge densities of the uncoated surfaces. The ratios of c_0 for $[\text{Fe}(\text{CN})_6]^{3-}$ and $[\text{Fe}(\text{CN})_6]^{4-}$ in Table I yield +0.45 and +0.2 e/nm² for bare of the chlorosilane and APTES surfaces, respectively, independent of w . With these values we calculate w from Eq. (2) to be 4 and 20 nm, respectively. Assuming $w = 4$ nm for trivalent ions screening silica, bare surface charge densities between -0.2 and -0.5 e/nm² are obtained for silica over the range of experimental conditions listed in Table I. These densities are in agreement with commonly accepted values [21].

The experimentally determined values of w are substantially higher than the simple estimate of $w = 0.3$ nm (the size of a water molecule) given by Shklovskii [9]. This difference represents an additional binding free energy of 2-4 kT for ions in the Stern layer. For $w = 0.2$ e/nm², the calculated value of c_0 corresponds to the lower end of the range of validity of Eq. (2), and this may be responsible for the larger discrepancy. There are also several approximations inherent in the simplified analytical theory. First, a primitive solvent model was used which neglects the structure of water and related hydration effects. Second, the surface charge was modelled as being uniformly distributed, whereas real surfaces consist of discrete chemical groups.

These experiments are among the first systematic steps toward understanding the fundamentals of screening of real surfaces by multivalent ions. Specific binding does not provide an adequate explanation for our observations, made in a regime where conventional mean-field theories have been predicted to break down. An alternative description based on ion correlations provides qualitative and semi-quantitative agreement with observations. In the future, measurements using electrostatic gating will allow tuning the surface charge density, permitting further quantitative tests of the theoretical predictions.

We thank J. Lyklema for useful discussions and C. Dekker for general support and useful discussions. This

work was supported by the 'Stichting voor Fundamenteel Onderzoek der Materie' (FOM) and the 'Netherlands Organization for Scientific Research' (NWO).

- [1] V. A. Bloomfield, *Biopolymers* 44, 269 (1998).
- [2] T. E. Angelini et al., *PNAS* 100, 8634 (2003).
- [3] R. O. James and T. W. Healey, *J. Coll. Int. Sci.* 40, 42 (1972); *J. Coll. Int. Sci.* 40, 53 (1972); *J. Coll. Int. Sci.* 40, 65 (1972).
- [4] A. M. Martin-Molina et al., *J. Chem. Phys.* 118, 4183 (2003).
- [5] R. M. Pashley, *J. Coll. Int. Sci.* 102, 23 (1984).
- [6] K. B. Agashe and J. R. Regalbuto, *J. Coll. Int. Sci.* 185, 174 (1996).
- [7] V. V. Iithayaveroj, S. Yiacoumi, and C. T. Souris, *J. Disp. Sci. Technol.* 24, 517 (2003).
- [8] For comprehensive reviews see A. Yu. Grosberg, T. T. Nguyen, and B. I. Shklovskii, *Rev. Mod. Phys.* 74, 329 (2002); Y. Levin, *Rep. Prog. Phys.* 65, 1577 (2002); M. Quesada-Perez et al., *Chem. Phys. Chem.* 4, 234 (2003).
- [9] B. I. Shklovskii, *Phys. Rev. E* 60, 5802 (1999).
- [10] W. A. Ducker, T. J. Senden, and R. M. Pashley, *Langmuir* 8, 1831 (1992).
- [11] Sum of metal ion radius and ligand (H_2O , NH_3 , CN^-) diameter. The radii are comparable (within 4%) to crystallographic data.
- [12] R. D. Shannon, *Acta Cryst. A* 32, 751 (1976).
- [13] Y. M. Marcus, *Ion properties* (Marcel Dekker Inc., New York, 1997), chapter 3.
- [14] All measurements were done at pH less than the first hydrolysis constant of the ions; J. Burgess, *Metal ions in solution* (Ellis Horwood, Chichester, England, 1979), chapter 9.
- [15] From crystal structure with van der Waals radii; A. Bacchi, F. Ferranti, and G. Pelizzetti, *Acta Cryst. C* 49, 1163 (1993).
- [16] Supporting electrolyte was a 1 mM HEPES (4-(2-hydroxyethyl)piperazine-1-ethanesulfonic acid) buffer, pH 7.0-0.3 set by adding KOH.
- [17] Supporting electrolyte was a mixture of 0.3 mM KOH and HCl with pH 6.5-0.5.
- [18] Supporting electrolyte was a mixture of 0.3 mM KOH and HCl with pH 5.8-0.3.

[19] Using 74 pm for Ru²⁺ radius, extrapolated from Ru^{3+ =4+ =5+} data [12].

[20] Supporting electrolyte was a 0.1 mM MES (2-morpholinoethanesulfonic acid) buffer, pH 6.0. 0.3 set by

adding KOH.

[21] R.K. Iler, *The chemistry of silica* (John Wiley and Sons, Inc., 1979).